analytical chemistry

Article

Cite This: Anal. Chem. 2019, 91, 15293−15299

pubs.acs.org/ac

Screen-Printed Carbon Electrodes Modified with Graphene Oxide for the Design of a Reagent-Free NAD$^+$-Dependent Biosensor Array

Johanna Pilas,[†,‡] Thorsten Selmer,[†] Michael Keusgen,[‡] and Michael J. Schöning*[,†,§]

[†]Institute of Nano- and Biotechnologies (INB), FH Aachen, Jülich, Germany

[‡]Institute of Pharmaceutical Chemistry, Philipps-Universität Marburg, Marburg, Germany

[§]Institute of Complex Systems 8 (ICS-8), Forschungszentrum Jülich, Jülich, Germany

ABSTRACT: A facile approach for the construction of reagent-free electrochemical dehydrogenase-based biosensors is presented. Enzymes and cofactors (NAD$^+$ and $Fe(CN)_6^{3-}$) were immobilized by modification of screen-printed carbon electrodes with graphene oxide (GO) and an additional layer of cellulose acetate. The sensor system was exemplarily optimized for an L-lactate electrode in terms of GO concentration, working potential, and pH value. The biosensor exhibited best characteristics at pH 7.5 in 100 mM potassium phosphate buffer at an applied potential of +0.250 V versus an internal pseudo Ag reference electrode. Thereby, sensor performance was characterized by a linear working range from 0.25 to 4 mM and a sensitivity of 0.14 μA mM^{-1}. The detection principle was additionally evaluated with three other dehydrogenases (D-lactate dehydrogenase, alcohol dehydrogenase, and formate dehydrogenase, respectively). The developed reagentless biosensor array enabled simultaneous and cross-talk free determination of L-lactate, D-lactate, ethanol, and formate.

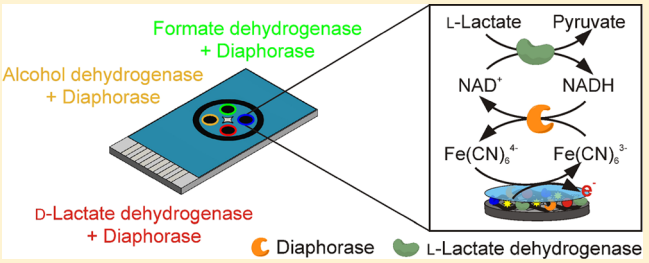

Nicotinamide adenine dinucleotide (NAD$^+$) plays an important role as an oxidizing agent in many central metabolic pathways. Thereby, the cofactor is involved in the electron transfer of dehydrogenase-catalyzed reactions.[1] Due to the great number of potentially available NAD$^+$-dependent dehydrogenases for a variety of analytes, this group of enzymes has been of special interest for the design of electrochemical biosensors within the last decades.[2,3] However, application of these enzymes, as biological recognition elements, is characterized by two main restrictions.[4] On the one hand, high overpotentials are required for direct oxidation of NADH, causing interference by oxidation of other electroactive species and electrode fouling.[5] Different approaches for a mediated electron transfer are reported in the literature in order to diminish this aspect by use of mediator compounds[6,7] or enzymes, like NADH oxidase[8,9] or diaphorase.[10,11] On the other hand, dehydrogenase-based biosensors depend on the permanent presence of the cofactor NAD$^+$. This circumstance makes the design of such devices more challenging. For this reason, great efforts have been made for the construction of reagent-free systems. Efficient coimmobilization of enzymes, cofactors, and mediators has been described with, for example, functionalized carbon nanotubes,[12−14] entrapment in carbon pastes,[15,16] membranes,[17,18] polypyrrol,[19,20] or chitosan films.[21,22]

Generally, research in this area focuses mainly on the development of single-analyte biosensors. For clinical, pharmaceutical, and environmental samples, however, often the simultaneous detection of more metabolites is of interest.[23,24] In this regard, application of arrays for several analytes seems advantageous.

Screen-printing technology facilitates cost-efficient production of disposable biosensing systems with the potential of flexible array design.[25,26] An amperometric biosensor for simultaneous determination of glucose and lactate was, for example, realized by modification of screen-printed carbon electrodes (SPCEs) with glucose oxidase and lactate oxidase, respectively.[27] Consideration of cross-talk effects is crucial for the fabrication of multianalyte devices. In order to minimize this aspect, two different sensing strategies have been used for dual monitoring of glucose and lactate by immobilizing glucose dehydrogenase and lactate oxidase on the working electrodes.[28] Additionally, the electrode surfaces were modified with graphene oxide (GO) for improvement of the electron transfer. Numerous studies have demonstrated the enhanced electrocatalytic activity of electrochemical biosensors functionalized with this biocompatible nanomaterial.[29,30]

Our group recently presented different multiparameter biosensors based on platinum thin-film electrodes for detection of various analytes.[31−34] However, these systems still depend on the addition of the cofactor NAD$^+$ to the measurement solution. The present work describes a facile approach for the development of reagentless dehydrogenase-based biosensors using SPCEs modified with GO and nafion (Figure 1). The system was evaluated using the example of an L-lactate

Received: October 1, 2019
Accepted: November 1, 2019
Published: November 1, 2019

DOI: 10.1021/acs.analchem.9b04481
Anal. Chem. 2019, 91, 15293−15299

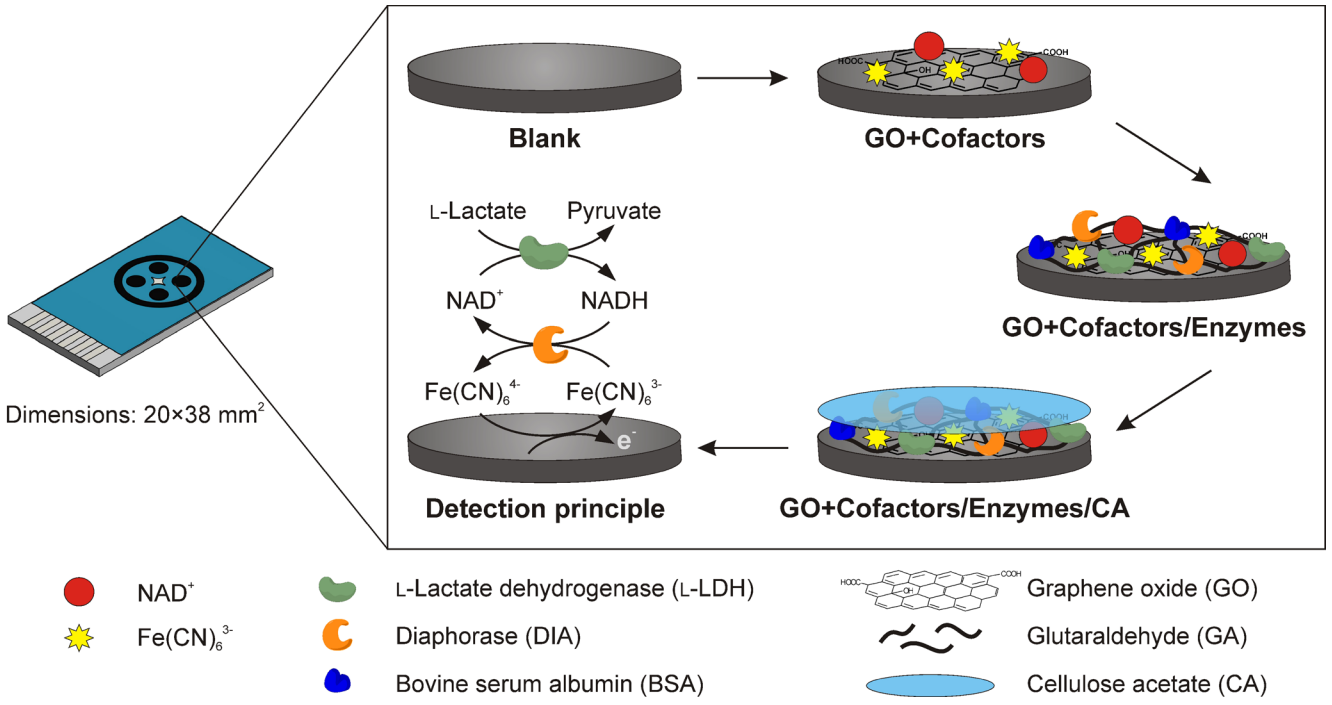

Figure 1. Schematic illustration of the multianalyte screen-printed carbon biosensor array. Extension shows exemplarily for the L-lactate sensor the different modification steps of the electrode surface and the detection principle.

dehydrogenase for construction of an electrochemical L-lactate electrode. The sensor performance was optimized with regard to the GO concentration, applied working potential, and pH value of the buffer solution. Additionally, the proposed sensor platform was examined with other dehydrogenases. In this way, a multianalyte biosensor array for simultaneous and cross-talk free determination of the metabolites L-lactate, D-lactate, ethanol, and formate was designed.

EXPERIMENTAL SECTION

Chemicals and Solutions. Bovine serum albumin (BSA), cellulose acetate (CA), ethanol, glutaraldehyde (GA, 25% in H_2O), glycerol, graphene oxide (GO, 4 mg mL^{-1} in H_2O), nafion, potassium ferricyanide ($K_3[Fe(CN)_6]$), and sodium D-lactate were obtained from Sigma-Aldrich. The cofactor NAD^+ and the substrates sodium formate and sodium L-lactate were purchased from AppliChem. Buffer components (K_2HPO_4, KH_2PO_4, and Tris-HCl) were from Carl Roth.

The enzymes alcohol dehydrogenase (ADH, 310U mg^{-1} from *Saccharomyces cerevisiae*), diaphorase (DIA, 51U mg^{-1} from *Clostridium kluyveri*), formate dehydrogenase (FDH, 0.49 U mg^{-1} from *Candida boidinii*), D-lactate dehydrogenase (D-LDH, 213 U mg^{-1} from *Lactobacillus leichmanii*), and L-lactate dehydrogenase (L-LDH, 174.5 U mg^{-1} from *Bacillus stearothermophilus*) were supplied from Sigma-Aldrich. All enzyme solutions were prepared in potassium phosphate buffer (100 mM, pH 7.5) and the enzymatic activity was determined photometrically in solution, as described earlier.[35] Enzyme loadings mentioned refer to the total amount of enzyme immobilized on the electrode surface.

Sensor Modification. Screen-printed carbon array electrodes were purchased from DropSens (ref 4W110). The sensor displayed four WEs (each Ø 2.95 mm) sharing one common carbon counter electrode (CE) and a silver pseudoreference electrode (RE). Figure 1 shows a schematic illustration of the sensor layout and the different steps used for construction of a reagent-less dehydrogenase-based L-lactate biosensor. Prior to modification, the sensor surface was electrochemically activated at +1.4 V for 240 s in 100 mM KCl.[36] GO (1.25 mg mL^{-1}) was dispersed in 100 mM potassium phosphate buffer (pH 7.5) by ultrasonication for 30 min and afterward, mixed with the cofactors (10 mM NAD^+, 20 mM $K_3[Fe(CN)]_6$) and 0.625% nafion. 4 μL of this solution were dropped on the electrode surface, and air-dried at room temperature. In the next step, the electrode was modified with the enzymes (1.5U L-LDH and 6.0U DIA). For improved enzyme immobilization within the GO matrix, the solution was enriched with 0.3% GA and 2% BSA. Finally, 3 μL of 1.2% CA (in acetone) were drop-coated on top of the enzyme membrane. The electrode was dried and kept at 4 °C when not in use.

The multianalyte biosensor array for the simultaneous measurement of L-lactate, D-lactate, formate, and ethanol was realized by immobilizing a different dehydrogenase on one of the four working electrodes (WEs). The enzyme loading of the D-lactate and formate electrodes was the same as described above (each 1.5U of D-LDH and FDH, respectively). In case of the ethanol electrode, a dehydrogenase loading of 16U ADH was used, since earlier studies revealed loss in enzyme activity after immobilization with the cross-linking agent GA.[35,37]

Apparatus. Electrochemical measurements were performed with a potentiostat with an integrated multiplexer (EmStatMUX16, PalmSens), which allows simultaneous analysis of up to 16 WEs. For all the experiments a conventional three-electrode arrangement was applied, consisting of the electrodes (4 WEs, CE, and RE) integrated on the SPCE array. Chronoamperometric studies were conducted at room temperature in a stirred solution of 10 mL potassium phosphate buffer (100 mM, pH 7.5) with an applied working potential of +0.250 V. For calibration of the different enzyme-

DOI: 10.1021/acs.analchem.9b04481
Anal. Chem. 2019, 91, 15293−15299

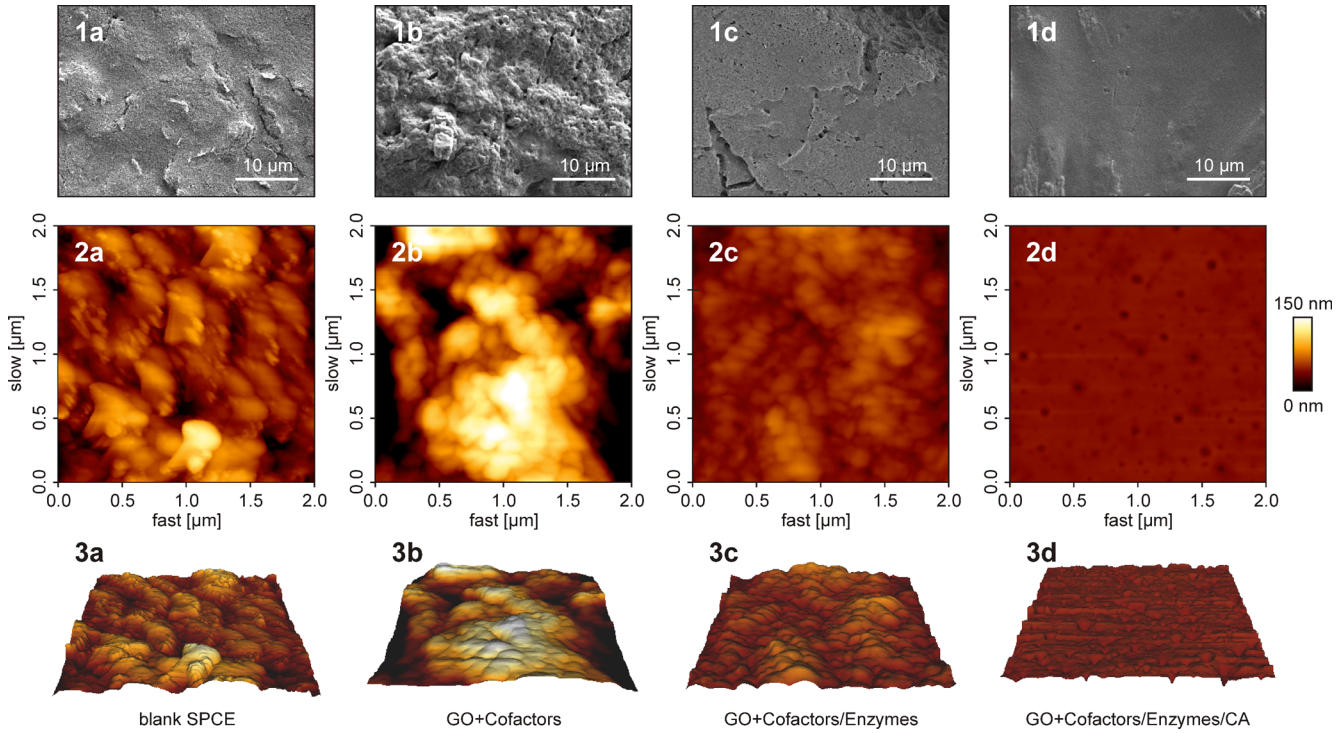

Figure 2. SEM images (1), AFM height (2), and three-dimensional profiles (3) of the blank SPCE (a), modified with GO and the cofactors (b), an additional layer of the enzymes L-LDH and DIA (c) and a membrane of CA (d). The scanned area of the AFM images was 2 × 2 μm^2.

modified electrodes, the increase in the current to stepwise addition of 40 mM analyte stock solution (L-lactate, D-lactate, formate, and ethanol, respectively) was recorded.

Cyclic voltammetry was carried out in the potential range between −0.4 and +0.8 V at a scan rate of 0.1 V s^{-1} in 100 mM potassium phosphate buffer (pH 7.5).

RESULTS AND DISCUSSION

Surface Characterization. The electrode surface was characterized by scanning electron microscopy (SEM) and atomic force microscopy (AFM), in order to evaluate the alterations in the morphology after each modification step. Figure 2.1a–d shows SEM images taken with a Jeol JSM-7800F (JEOL GmbH, Germany). Compared to the bare SPCE (Figure 2.1a), the morphology of the electrode modified with GO and the cofactors was characterized by a rougher surface with some porosity (Figure 2.1b). After immobilization of the enzymes with GA within the porous GO matrix, the surface appears relatively smooth, as displayed in Figure 2.1c. In comparison to the enzyme layer, the CA membrane exhibits an even smoother morphology with a denser matrix (Figure 2.1d).

Figure 2.2a–d and Figure 2.3a–d represent AFM height profiles and three-dimensional images, respectively, taken in the tapping mode with silicon cantilevers (Arrow NCR, NanoWorld AG, Switzerland) using a BioMat Workstation (JPK Instruments, Germany). The surface roughness was determined in terms of root-mean-square (RMS) roughness. The untreated SPCE exhibited a RMS of 16.5 ± 4.4 nm. After application of GO, the roughness increased to 37.8 ± 5.9 nm. Further modification steps resulted in a lower RMS of 9.2 ± 1.3 and 2.3 ± 0.7 nm of the enzyme membrane and the CA layer, respectively. These findings are consistent with the SEM images, as described above.

Optimization of the Current Response. *GO Concentration.* The protocol for the electrode modification was optimized in regard to the applied GO concentration. For this reason, the effect of the GO loading on the immobilization of the cofactors was evaluated by cyclic voltammetry. Figure 3

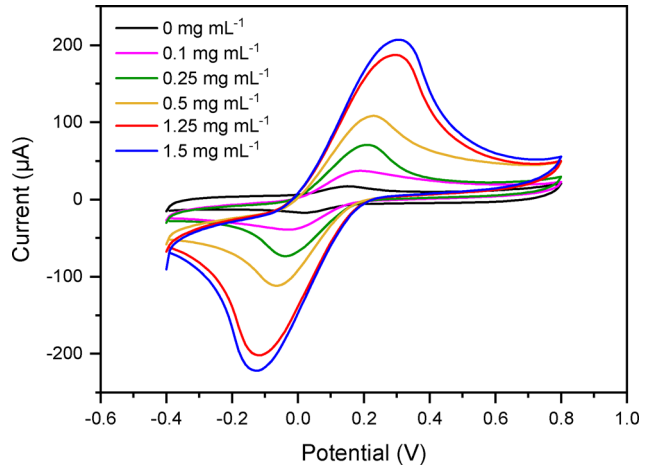

Figure 3. Cyclic voltammograms of SPCEs modified with $Fe(CN)_6^{3-}$, NAD^+, and different concentrations of GO 0–1.5 mg mL^{-1}. Measurements were performed in 100 mM potassium phosphate buffer (pH 7.5).

shows the cyclic voltammograms obtained with GO concentrations in the range from 0 to 1.5 mg mL^{-1}. All curves exhibited the typical cyclic voltammogram characteristic for the reversible reduction of $Fe(CN)_6^{3-}$ to $Fe(CN)_6^{4-}$ with increasing potential.[38,39] Thereby, a higher current for the oxidation peak was observed with increasing GO loading. These results demonstrate the enhanced electrocatalytic

DOI: 10.1021/acs.analchem.9b04481
Anal. Chem. 2019, 91, 15293−15299

activity of the SPCEs modified with GO. Various studies demonstrated superior electrochemical properties of different electrode materials (such as SPCEs,[40,41] glassy carbon electrodes,[42,43] and platinum electrodes[44]) by modification with GO and nafion. The electrode modified with 1.5 mg mL^{-1} GO displayed the highest current response. However, the high GO amount hindered homogeneous distribution of the solution on the electrode surface and uniform drying. So, for further experiments, a concentration of 1.25 mg mL^{-1} GO was chosen.

Working Potential. The optimal working conditions for amperometric detection of L-lactate were additionally examined in terms of the applied working potential and the pH value of the measurement solution. In Figure 4, the

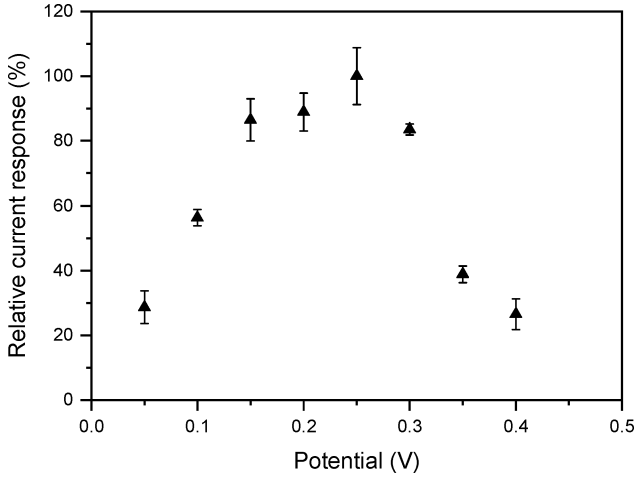

Figure 4. Influence of the applied working potential on the amperometric response of the L-lactate electrode modified with 1.25 mg mL^{-1} GO to 1 mM L-lactate in 100 mM potassium phosphate buffer (pH 7.5). Relative current response represents the signal normalized to the maximum obtained current.

relationship between the relative current response after the addition of 1 mM L-lactate and the potential applied to the WE is depicted. The signal was normalized to the maximum obtained current change. The highest signal increase was observed at a potential of +0.250 V versus the internal pseudo silver reference electrode. At more positive potentials, the amperometric signal decreased to about 26.5% at +0.4 V. These results are in good agreement with the typical redox potentials of the $Fe(CN)_6^{3-}/Fe(CN)_6^{4-}$ system, as visualized by the cyclovoltamograms in Figure 3. Similar optimal potentials are reported in the literature for electrochemical biosensors based on the mediated electron transfer of the redox couple $Fe(CN)_6^{3-}/Fe(CN)_6^{4-}$.[11,45] Thus, for further studies, a working potential of +0.250 V was selected.

pH of the Buffer Solution. The characteristics of the surrounding environment have a great impact on the catalytic activity of enzymes, which determines mainly the overall biosensor sensitivity. For this reason, the dependence of the amperometric response on the pH value of the measurement solution was studied over the range from pH 6.0 to 8.0 in potassium phosphate buffer and from pH 8.5 to 9.0 in Tris-HCl buffer. As presented in Figure 5, the current increased with increasing pH value, reaching a maximum signal in phosphate buffer at pH 7.5. Measurements at higher pH values resulted in lower change in the current signal. This

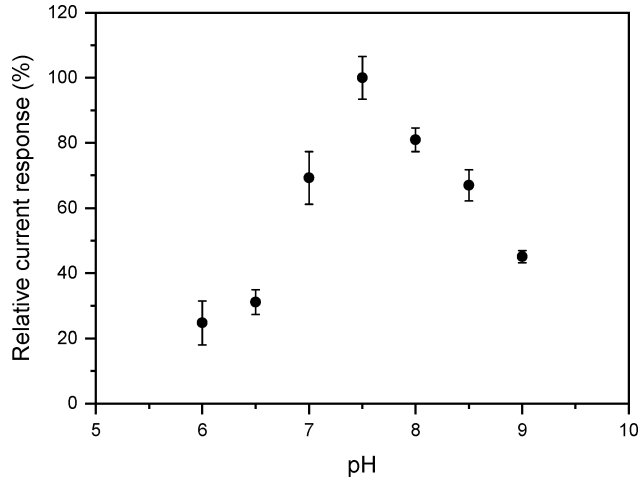

Figure 5. Effect of pH on the amperometric sensor response. Experiments were carried out in 100 mM potassium phosphate buffer (pH 6.0–8.0) and Tris-HCl buffer (pH 8.5–9.0) at an applied working potential of +0.250 V. Relative current response represents the signal increase after addition of 1 mM L-lactate, normalized to the maximum obtained current.

characteristic is consistent with other L-lactate biosensors described in literature that also utilize L-LDHs in combination with DIA[11,35,46] or an alternative approach for electrochemical detection of L-lactate.[47,48] Hence, further experiments were conducted at pH 7.5 in phosphate buffer.

Amperometric Detection of L-Lactate. The effect of each component (cofactors, GO and CA, respectively) on the electrochemical electrode response was investigated by modification of the SPCE with different membrane compositions. Figure 6 shows the individual amperometric signal of each electrode to the successive addition of L-lactate in the concentration range from 0.25 to 6 mM. The curve in Figure 6a represents an GO/Enzymes/CA electrode that has been constructed without the cosubstrates NAD^+ and $Fe(CN)_6^{3-}$. In this case, no change in the current occurred after stepwise increase of the L-lactate concentration. This observation proves that both cofactors are essentially required for the enzymatic reaction, as depicted in Figure 1, and thus, for the amperometric detection principle. In comparison, modification of the electrode surface with cofactors/enzymes/CA (b) resulted in a stepwise increase in the current response each time the analyte is added to the measurement solution. However, the final three concentrations steps (3, 4, and 6 mM) are accompanied by a gradual decrease of the amperometric signal, probably due to leakage of one or both of the cofactors from the sensor surface. The improved immobilization of the cofactors by modification of the electrode with GO is revealed by curve Figure 6c,d. The electrode modified with GO, but without CA (see Figure 6c GO+Cofactors/Enzymes), showed a continuous increase of current with increasing L-lactate concentration. This was also the case for the GO+Cofactors/Enzymes/CA electrode (d). For both electrodes, a stable signal response over the whole measurement time was obtained. This might be due to an enhanced immobilization of the required cosubstances by integration of GO on the sensor surface, compared to the electrode prepared without GO (Figure 6a). The insets in Figure 6 display the corresponding calibration curves of the different electrodes. The sensitivities obtained for the Cofactors/Enzymes/CA, GO+Cofactors/Enzymes, and

DOI: 10.1021/acs.analchem.9b04481
Anal. Chem. 2019, 91, 15293−15299

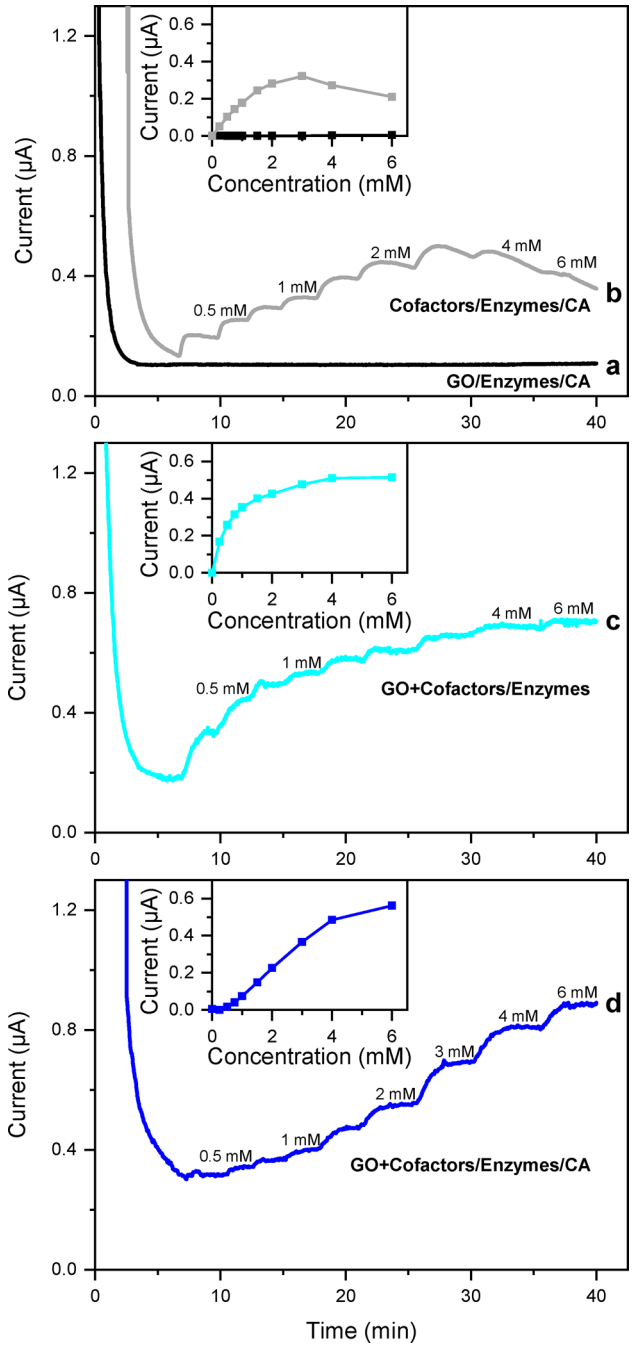

Figure 6. Amperometric response of SPCEs with different electrode modifications (GO/Enzymes/CA (a), Cofactors/Enzymes/CA (b), GO+Cofactors/Enzymes (c), and GO+Cofactors/Enzymes/CA (d)) to the successive addition of L-lactate (0.25−6 mM). Measurements were performed in 100 mM phosphate buffer (pH 7.5) at an applied potential of +0.250. Insets show the corresponding calibration curves as a function of L-lactate concentration.

GO+Cofactors/Enzymes/CA electrode were 0.16, 0.51, and 0.14 μA mM^{-1}, respectively. Thereby, the GO+Cosubstrates/Enzymes/CA electrode (d) exhibited the broadest linear range from 0.25 to 4.0 mM. These results demonstrated that with an additional CA layer the linear detection range can be extended, as also described by other electrochemical enzyme-based biosensors.[49,50] The permselective membrane serves as a diffusion barrier, which hinders the transport of the analyte to the electrode surface. Consequently, the sensitivity of the SPCE is influenced. The application of such membranes is also commonly used in order to reduce the impact of other electroactive species in complex sample solutions.[51]

Reagent-Free Biosensor Array for Simultaneous Measurement. The applicability of the developed reagent-free sensor platform was evaluated with three other dehydrogenases. For construction of D-lactate-, formate-, and ethanol-sensitive electrodes, D-LDH, FDH, and ADH, respectively, were used for sensor modification, as described earlier. First, each electrode was calibrated by amperometric measurements with the corresponding analyte. Table 1 summarizes obtained characteristics of the different electrodes in terms of the linear working range and sensitivity. In comparison, the ethanol sensor exhibited the highest sensitivity with 1.07 μA mM^{-1}. These performances proved that the detection principle, in combination with the electrode modification, is generally applicable to different NAD$^+$-dependent dehydrogenases.

Table 1. Characteristics of the Individual Electrodes of the Reagentless Multianalyte SPCE Array

analyte	linear range (mM)	sensitivity (μA mM^{-1})
L-lactate	0.25−4.0	0.14
D-lactate	0.25−4.0	0.18
ethanol	0.05−2.0	1.07
formate	0.25−4.0	0.09

In order to evaluate potential cross-talk effects between electrodes modified with different dehydrogenases, a multianalyte biosensor was constructed. Figure 7 illustrates an amperometric measurement of four analytes at the same applied potential of +0.250 V. The capability of cross-talk free detection is demonstrated by consecutive titration of each analyte individually (D-lactate, L-lactate, formate, and ethanol, respectively). In each case, the addition of the particular analyte results in an increase in the current signal of only the corresponding dehydrogenase electrode, while the other ones remain constant. The capability of simultaneous analysis of all four different analytes is substantiated by the last two titration steps, in which a multicomponent solution was used. Hereby, all four electrodes responded with an increase in the electrochemical signal due to increasing analyte concentration, according to the specific sensitivity for each electrode.

CONCLUSIONS

The modification of SPCE with GO has provided a simple technique for construction of reagentless NAD$^+$-dependent biosensors. In this study, this platform has been evaluated by the development of an electrochemical enzyme-based L-lactate biosensor. The immobilization of the cofactors NAD$^+$ and $Fe(CN)_6^{3-}$ on the electrode surface has been achieved by functionalization with GO and an additional layer of CA. Thereby, the amperometric signal response was optimized in regard to GO concentration, working potential, and pH of the buffer solution. Experiments revealed that best results were obtained at an applied potential of +0.250 V in 100 mM potassium phosphate buffer at pH 7.5. Furthermore, the proposed reagent-free biosensing system has been successfully tested with three other NAD$^+$-dependent dehydrogenases. In this way, a multianalyte biosensor for simultaneous determination of L-lactate, D-lactate, ethanol, and formate was fabricated based on an SPCE array. This device enabled

DOI: 10.1021/acs.analchem.9b04481
Anal. Chem. 2019, 91, 15293−15299

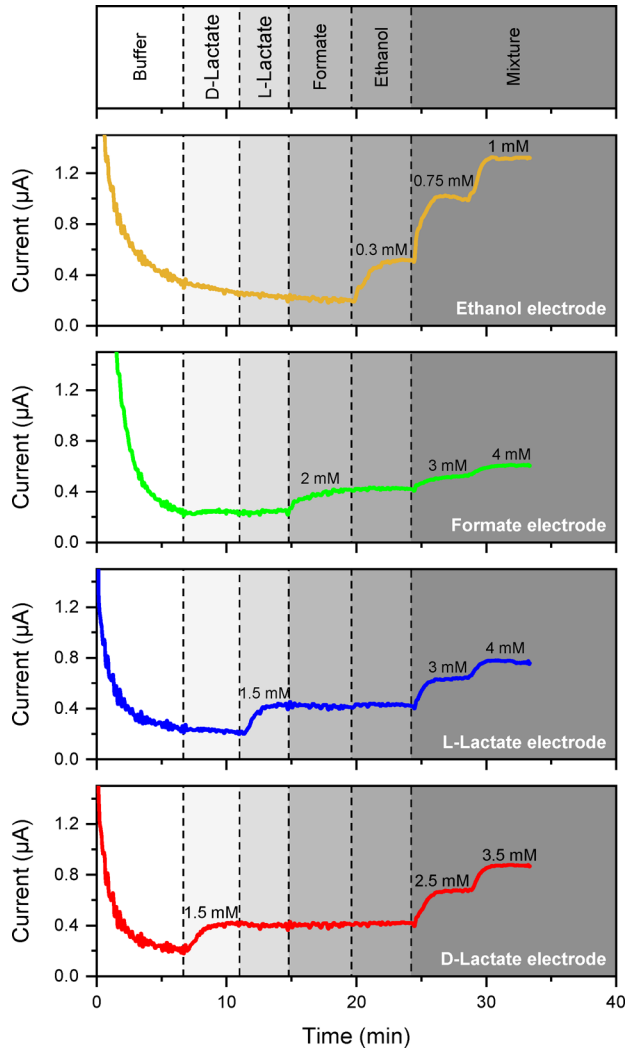

Figure 7. Simultaneous amperometric responses of the reagent-less multianalyte SPCE array to successive addition of D-lactate, L-lactate, formate, ethanol, and a mixture of all four analytes. Measurement was performed in 100 mM potassium phosphate buffer (pH 7.5) at an applied potential of +0.250 V.

cross-talk free amperometric detection of four analytes without the requirement of adding external NAD^+ and mediator to the measurement solution. The present work demonstrates the promising potential of a disposable biosensor array characterized by facile application and rapid analysis. Such system could, for example, be used for the monitoring of fermentation processes, where knowledge about the concentration profile of different analytes is of great importance. In this regard, future work concentrates on the improvement of the sensor performance and evaluation of the stability in complex biological samples such as fermentation broth.

AUTHOR INFORMATION

Corresponding Author

*E-mail: schoening@fh-aachen.de. Phone: +49 (0)241 6009 53144. Fax: +49 (0)241 6009 53229.

ORCID

Johanna Pilas: 0000-0002-6408-9978

Notes

The authors declare no competing financial interest.

ACKNOWLEDGMENTS

The authors thank J. Arreola for the AFM measurements and D. Rolka for the SEM images.

REFERENCES

(1) Sellés Vidal, L.; Kelly, C. L.; Mordaka, P. M.; Heap, J. T. *Biochim. Biophys. Acta, Proteins Proteomics* **2018**, *1866*, 327−347.
(2) Katakis, I.; Domínguez, E. *Microchim. Acta* **1997**, *126*, 11−32.
(3) Lobo, M. J.; Miranda, A. J.; Tuñón, P. *Electroanalysis* **1997**, *9*, 191−202.
(4) Radoi, A.; Compagnone, D. *Bioelectrochemistry* **2009**, *76*, 126−137.
(5) Blaedel, W. J.; Jenkins, R. A. *Anal. Chem.* **1975**, *47*, 1337−1343.
(6) Gorton, L.; Dominguez, E. *Rev. Mol. Biotechnol.* **2002**, *82*, 371−392.
(7) Kochius, S.; Magnusson, A. O.; Hollmann, F.; Schrader, J.; Holtmann, D. *Appl. Microbiol. Biotechnol.* **2012**, *93*, 2251−2264.
(8) Leca, B.; Marty, J.-L. *Biosens. Bioelectron.* **1997**, *12*, 1083−1088.
(9) Montagné, M.; Erdmann, H.; Comtat, M.; Marty, J.-L. *Sens. Actuators, B* **1995**, *27*, 440−443.
(10) Limoges, B.; Marchal, D.; Mavré, F.; Savéant, J.-M. *J. Am. Chem. Soc.* **2006**, *128*, 2084−2092.
(11) Antiochia, R.; Cass, A.; Palleschi, G. *Anal. Chim. Acta* **1997**, *345*, 17−28.
(12) Zhou, H.; Zhang, Z.; Yu, P.; Su, L.; Ohsaka, T.; Mao, L. *Langmuir* **2010**, *26*, 6028−6032.
(13) Gallay, P.; Eguílaz, M.; Rivas, G. *Electroanalysis* **2019**, *31*, 805−812.
(14) Khorsand, F.; Darziani Azizi, M.; Naeemy, A.; Larijani, B.; Omidfar, K. *Mol. Biol. Rep.* **2013**, *40*, 2327−2334.
(15) Shu, H. C.; Mattiasson, B.; Persson, B.; Nagy, G.; Gorton, L.; Sahni, S.; Geng, L.; Boguslavsky, L.; Skotheim, T. *Biotechnol. Bioeng.* **1995**, *46*, 270−279.
(16) Weiss, D. J.; Dorris, M.; Loh, A.; Peterson, L. *Biosens. Bioelectron.* **2007**, *22*, 2436−2441.
(17) Blaedel, W. J.; Engstrom, R. C. *Anal. Chem.* **1980**, *52*, 1691−1697.
(18) Maines, A.; Prodromidis, M. I.; Tzouwara-Karayanni, S. M.; Karayannis, M. I.; Ashworth, D.; Vadgama, P. *Anal. Chim. Acta* **2000**, *408*, 217−224.
(19) Pereira, A. *Talanta* **2001**, *53*, 801−806.
(20) Gros, P.; Comtat, M. *Biosens. Bioelectron.* **2004**, *20*, 204−210.
(21) Zhang, M.; Gorski, W. *Electroanalysis* **2011**, *23*, 1856−1862.
(22) Hughes, G.; Pemberton, R. M.; Fielden, P. R.; Hart, J. P. *Sens. Actuators, B* **2015**, *216*, 614−621.
(23) Justino, C. I. L.; Duarte, A. C.; Rocha-Santos, T. A. P. *Sensors* **2017**, *17*, 2918.
(24) Davis, A. N.; Travis, A. R.; Miller, D. R.; Cliffel, D. E. *Annu. Rev. Anal. Chem.* **2017**, *10*, 93−111.
(25) Couto, R.; Lima, J.; Quinaz, M. B. *Talanta* **2016**, *146*, 801−814.
(26) Hughes, G.; Westmacott, K.; Honeychurch, K. C.; Crew, A.; Pemberton, R. M.; Hart, J. P. *Biosensors* **2016**, *6*, 50.
(27) Sato, N.; Okuma, H. *Anal. Chim. Acta* **2006**, *565*, 250−254.
(28) Kanso, H.; Begoña González García, M.; Ma, S.; Ludwig, R.; Fanjul Bolado, P.; Hernández Santos, D. *Electroanalysis* **2017**, *29*, 87−92.
(29) Kuila, T.; Bose, S.; Khanra, P.; Mishra, A. K.; Kim, N. H.; Lee, J. H. *Biosens. Bioelectron.* **2011**, *26*, 4637−4648.
(30) Song, Y.; Luo, Y.; Zhu, C.; Li, H.; Du, D.; Lin, Y. *Biosens. Bioelectron.* **2016**, *76*, 195−212.
(31) Pilas, J.; Iken, H.; Selmer, T.; Keusgen, M.; Schöning, M. J. *Phys. Status Solidi A* **2015**, *212*, 1306−1312.
(32) Röhlen, D. L.; Pilas, J.; Schöning, M. J.; Selmer, T. *Appl. Biochem. Biotechnol.* **2017**, *183*, 566−581.
(33) Pilas, J.; Yazici, Y.; Selmer, T.; Keusgen, M.; Schöning, M. J. *Sensors* **2018**, *18*, 1470.

DOI: 10.1021/acs.analchem.9b04481
Anal. Chem. 2019, 91, 15293−15299

(34) Röhlen, D. L.; Pilas, J.; Dahmen, M.; Keusgen, M.; Selmer, T.; Schöning, M. J. *Front. Chem.* **2018**, *6*, 284.
(35) Pilas, J.; Yazici, Y.; Selmer, T.; Keusgen, M.; Schöning, M. J. *Electrochim. Acta* **2017**, *251*, 256−262.
(36) Cui, G.; Yoo, J. H.; Lee, J. S.; Yoo, J.; Uhm, J. H.; Cha, G. S.; Nam, H. *Analyst* **2001**, *126*, 1399−1403.
(37) Mateo, C.; Palomo, J. M.; van Langen, L. M.; van Rantwijk, F.; Sheldon, R. A. *Biotechnol. Bioeng.* **2004**, *86*, 273−276.
(38) Rock, P. A. *J. Phys. Chem.* **1966**, *70*, 576−580.
(39) O'Reilly, J. E. *Biochim. Biophys. Acta, Bioenerg.* **1973**, *292*, 509−515.
(40) Brownson, D. A. C.; Banks, C. E. *Analyst* **2011**, *136*, 2084−2089.
(41) Vasilescu, I.; Eremia, S. A. V.; Penu, R.; Albu, C.; Radoi, A.; Litescu, S. C.; Radu, G.-L. *RSC Adv.* **2015**, *5*, 261−268.
(42) Li, J.; Guo, S.; Zhai, Y.; Wang, E. *Anal. Chim. Acta* **2009**, *649*, 196−201.
(43) Chen, X.; Ye, H.; Wang, W.; Qiu, B.; Lin, Z.; Chen, G. *Electroanalysis* **2010**, *22*, 2347−2352.
(44) Vinu Mohan, A. M.; Aswini, K. K.; Maria Starvin, A.; Biju, V. M. *Anal. Methods* **2013**, *5*, 1764−1770.
(45) Zeng, K.; Tachikawa, H.; Zhu, Z.; Davidson, V. L. *Anal. Chem.* **2000**, *72*, 2211−2215.
(46) Sprules, S. D.; Hart, J. P.; Wring, S. A.; Pittson, R. *Anal. Chim. Acta* **1995**, *304*, 17−24.
(47) Kwan, R. C. H.; Hon, P. Y. T.; Mak, K. K. W.; Renneberg, R. *Biosens. Bioelectron.* **2004**, *19*, 1745−1752.
(48) Pérez, S.; Sánchez, S.; Fàbregas, E. *Electroanalysis* **2012**, *24*, 967−974.
(49) Maines, A.; Ashworth, D.; Vadgama, P. *Anal. Chim. Acta* **1996**, *333*, 223−231.
(50) Kanapieniene, J. J.; Dedinaite, A. A.; Laurinavicius, V. A. *Sens. Actuators, B* **1992**, *10*, 37−40.
(51) Kulkarni, T.; Slaughter, G. *Membranes* **2016**, *6*, 55.

DOI: 10.1021/acs.analchem.9b04481
Anal. Chem. 2019, 91, 15293−15299